

# Characterizing and modeling cyclic behavior in non-stationary time series through multi-resolution analysis

Dilip P. Ahalpara\*

*Institute for Plasma Research, Near Indira Bridge, Gandhinagar-382428, India*

Amit Verma,<sup>†</sup> Prasanta K. Panigrahi,<sup>‡</sup> and Jitendra C. Parikh<sup>§</sup>

*Physical Research Laboratory, Navrangpura, Ahmedabad-380009, India*

(Dated: February 6, 2022)

A method based on wavelet transform and genetic programming is proposed for characterizing and modeling variations at multiple scales in non-stationary time series. The cyclic variations, extracted by wavelets and smoothened by cubic splines, are well captured by genetic programming in the form of dynamical equations. For the purpose of illustration, we analyze two different non-stationary financial time series, S&P CNX Nifty closing index of the National Stock Exchange (India) and Dow Jones industrial average closing values through Haar, Daubechies-4 and continuous Morlet wavelets for studying the character of fluctuations at different scales, before modeling the cyclic behavior through GP. Cyclic variations emerge at intermediate time scales and the corresponding dynamical equations reveal characteristic behavior at different scales.

PACS numbers: 05.45.Tp, 89.65.Gh

## I. INTRODUCTION

A number of non-stationary time series are known to comprise of fluctuations having both stochastic and cyclic or periodic components. Isolating fluctuations from these time series, at different scales for the purpose of characterization and modeling is a research area of significant interest [1, 2, 3]. Here we explicate a wavelet based approach for separating structured variations from the stochastic ones in a time series before modeling them through genetic programming (GP). For the purpose of illustration we have chosen two financial time series, since the same is well-known to exhibit random and structured behavior at different scales [4, 5]. At small time scales, the fluctuations are primarily stochastic in nature; at higher scales the random part is averaged out and characteristic nature of the variations become transparent. For a reliable analysis one also needs to have a reasonably long data set for which the financial time series are well suited. The chosen time series are S&P CNX Nifty closing index of the National Stock Exchange (India) and Dow Jones industrial average closing values, representing two sufficiently different economic climates so as to bring out the efficacy of the present approach.

Study and characterization of fluctuations in financial time series have been studied through a variety of approaches. For example, variations have been analyzed through Levy-stable non-Gaussian model [6]. Stochastic nature of the high frequency fluctuations and presence of structured behavior have emerged through study of

these time series using random matrix theory. In particular, analysis of the cross-correlations between different stocks [7, 8] reveal universal and non-universal phenomena. The latter ones indicate correlated behavior between stocks of different companies. This behavior can manifest in the composite stock price indices, where the correlated behavior of several companies can give rise to structured or cyclic behavior in appropriate time scales. Wavelet transform, because of its multi-resolution analysis property is well-suited to isolate fluctuations and variations at different scales [9, 10].

The goal of the present article is to demonstrate the usefulness of combining wavelet transform with tools like genetic programming for modeling of fluctuations. We carry out our analysis on two different financial time series, in order to find out the similarities and differences between them, from the perspective of fluctuations. Apart from sharp transients representing sudden variations ascribable to physical causes, the high frequency fluctuations at small scales are primarily random in character. In all the time series, cyclic behavior emerges at higher scales, when the random fluctuations are averaged out. The physical nature of the cyclic phenomena is substantiated through both discrete and continuous wavelets. In case of continuous wavelets, the scalogram clearly reveals cyclic behavior at intermediate scales. We then proceed to model these variations through Genetic Programming (GP) [11, 12, 13, 14, 15]. For that purpose, we smoothen the cyclic behavior at every scale, corresponding to different levels of wavelet decomposition, through a cubic spline. It needs to be mentioned that, since the purpose is to model cyclic behavior, physically it is meaningful to smoothen the same, before trying to model them.

We study the fluctuation characteristics of two different financial time series, S&P CNX Nifty closing index of the National Stock Exchange (India) and Dow Jones

\*Electronic address: dilip@ipr.res.in

<sup>†</sup>Electronic address: amit.verma@yahoo.com

<sup>‡</sup>Electronic address: prasanta@prl.res.in

<sup>§</sup>Electronic address: parikh@prl.res.in

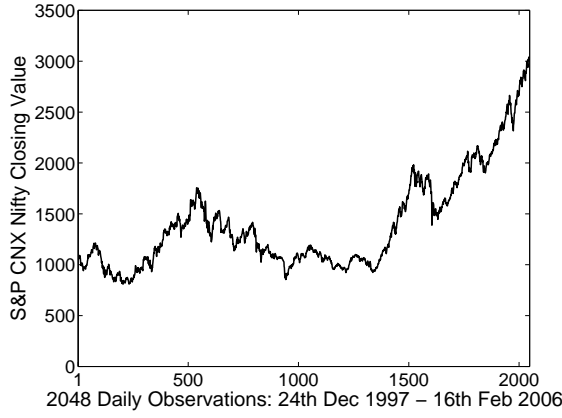


FIG. 1: S&P CNX Nifty closing index data having 2048 points covering the daily index lying within 24-Dec-1997 to 16-Feb-2006.

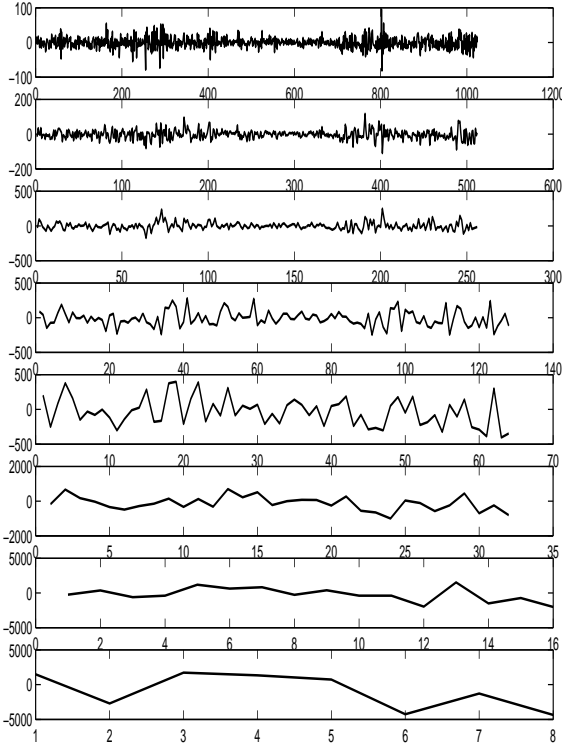


FIG. 2: Haar wavelet fluctuation coefficients for levels 1 to 8 for Nifty data. Transient and stochastic behavior at small scales and ordered variations at higher scales are evident.

industrial average closing values, through wavelet transforms belonging to both discrete and continuous families. Haar and Daubechies-4 (Db4) from the discrete wavelet family and the continuous Morlet wavelet are used to analyze the time series. As has been observed earlier, at small scales, the fluctuations captured by the wavelet coefficients exhibit self-similar character [16]. Clear cyclic behavior emerges in medium scales and is evident from both discrete and continuous wavelet analysis. It is found that, GP captures the cyclic behavior at each scale quite

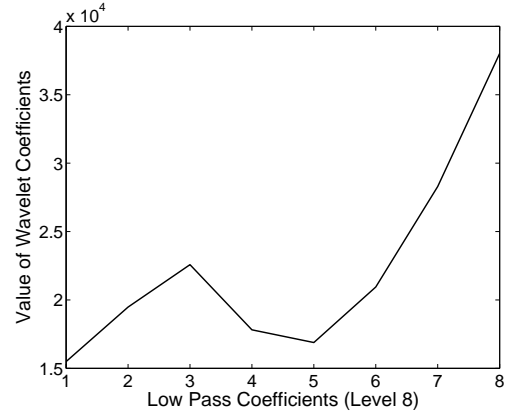


FIG. 3: Haar wavelet low pass coefficients for level 8 for Nifty data. As expected, these coefficients resemble the average behavior of the time series.

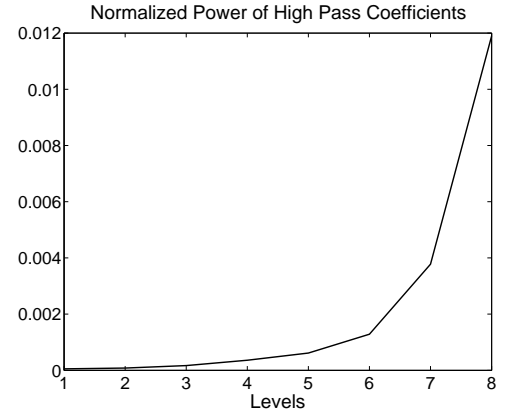


FIG. 4: Normalized power of Haar wavelet coefficients for different levels 1 to 8 for Nifty data. Indication of rapid increase from 6<sup>th</sup> level is clearly visible.

well. The dynamical equations are primarily linear with nonlinear additive terms of Padé type. These equations are checked for their predictive capabilities by making out-of-sample predictions. One-step out-of-sample predictions are made which use given time lagged values successively and predict the next data set value. It is found that the one-step predictions are very good.

The paper is organized as follows. In Section II, we give a brief introduction to wavelets before carrying out wavelet decomposition of both the data sets considered to study the character of the variations at different scales. Cyclic variations at different scales is extracted through Daubechies-4 wavelet and confirmed by continuous Morlet wavelet. We then proceed to model the cyclic phenomenon through GP in section III and conclude in section IV, after pointing out a number of applications and future directions of work through the present method.

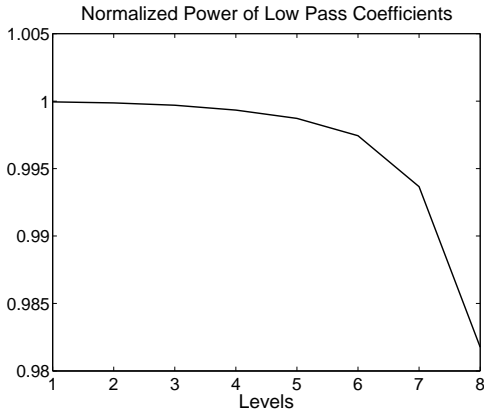


FIG. 5: Normalized power of Haar wavelet low pass coefficients for different levels 1 to 8 for Nifty data. One observes decrease in low-pass power from 6<sup>th</sup> level onwards.

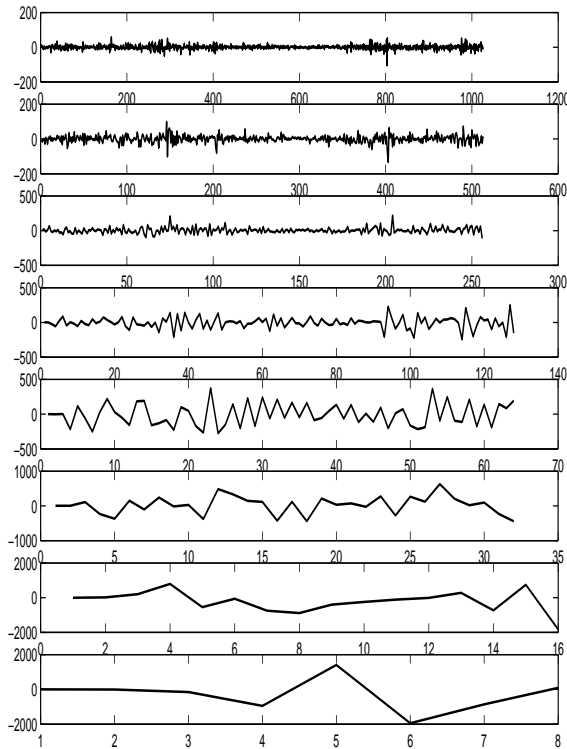


FIG. 6: Db4 Wavelet coefficients for different levels 1 to 8 for Nifty data. Cyclic behavior at intermediate scales are well captured by the wavelet coefficients. This behavior is present both at local and global levels.

## II. WAVELET TRANSFORM

Wavelet transform provides a powerful tool for the analysis of transient and non-stationary data and is particularly useful in picking out characteristic variations at different resolutions or scales [17]. In the context of financial time series [18, 19], it has found extensive applications. It has been used for the study of commodity prices [20], in measuring correlations [21], in the study

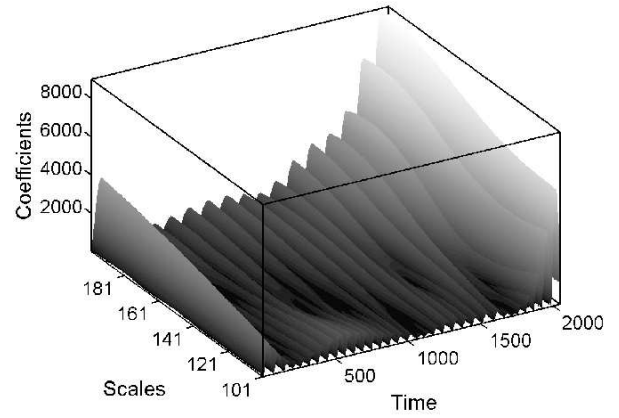


FIG. 7: Scalogram of Morlet wavelet coefficients for scales 101-200 of S&P CNX Nifty closing index values.

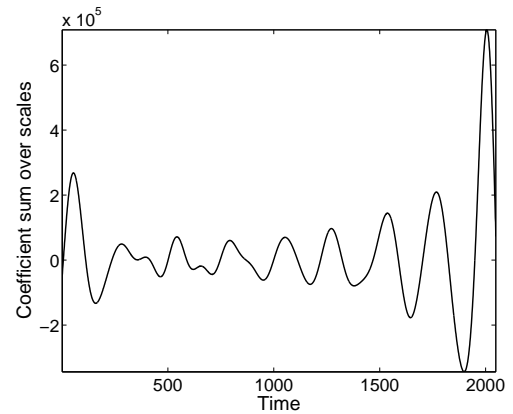


FIG. 8: Sum of wavelet coefficients for Nifty data over all scales as a function of time. An approximate periodic behavior with periodicity of about 200 trading days is evident.

of foreign exchange rates [22] and for predicting stock market behavior [23, 24], to name a few. This linear transform separates a data set in the form of low-pass or average coefficients, resembling the data itself, and wavelet or high-pass coefficients at different levels, which capture the variations at corresponding scales. Wavelets can be continuous or discrete. In the latter case, the basis elements are strictly finite in size, enabling them to achieve localization, while disentangling characteristic variations at different frequencies.

In discrete wavelet transform (DWT), the construction of basis set starts with the scaling function  $\varphi(x)$  (father wavelet) and the mother wavelet  $\psi(x)$ , whose height and width are arbitrary:  $\int \varphi dx = A$ ,  $\int \psi dx = 0$ ,  $\int \varphi \psi dx = 0$ ,  $\int |\varphi|^2 dx = 1$ ,  $\int |\psi|^2 dx = 1$ , where  $A$  is an arbitrary constant. The scaling and wavelet functions, and their scaled translates, known as daughter wavelets,  $\psi_{j,k} = 2^{j/2} \psi(2^j x - k)$ , are square integrable at different scales. Here,  $k$  and  $j$  respectively are the translation and scaling parameters, with  $-\infty \leq k \leq +\infty$ . Although conventionally, one starts with the scale value  $j = 0$ , one can begin from any finite value  $j'$  and increase it by in-

tegral units. The original mother wavelet corresponds to  $\psi_{0,0}$ . The daughter wavelets are of a similar form as the mother wavelet, except that their width and height differ by a factor of  $2^j$  and  $2^{j/2}$  respectively, at successive levels. The translation unit  $k/2^j$  is commensurate with the thinner size of the daughter wavelet at scale  $j$ . In the limit  $j \rightarrow \infty$ , these basis functions form a complete orthonormal set, allowing us to expand a signal  $f(t)$  in the form,

$$f(t) = \sum_{k=-\infty}^{+\infty} c_{j,k} \varphi_{j,k}(t) + \sum_{k=-\infty}^{+\infty} \sum_{j' \geq j} d_{j',k} \psi_{j',k}(t) \quad (1)$$

Here,  $c_{j,k}$ 's are the low-pass coefficients and  $d_{j,k}$ 's are the high-pass or wavelet coefficients. They respectively capture the average part and variations of the signal at scale  $j$  and location  $k$ . For the discrete wavelets, the property of multi-resolution analysis (MRA) leads to  $c_{j,k} = \sum_n h(n-2k)c_{j+1,n}$ ,  $d_{j,k} = \sum_n \tilde{h}(n-2k)c_{j+1,n}$ , where  $h(n)$  and  $\tilde{h}(n)$  are respectively the low-pass (scaling function) and high-pass (wavelet) filter coefficients, which differ for different wavelets. Both low-pass and high-pass coefficients at a scale  $j$  can be obtained from the low-pass coefficients at a higher scale ( $c_{j+1,n}$ ). This implies that, starting from the finest resolution of the signal, one can construct both scaling and wavelet coefficients, by convolution with the filter coefficients  $h(n)$  and  $\tilde{h}(n)$ .

For the Haar wavelet:  $h(0) = h(1) = \frac{1}{\sqrt{2}}$  and  $\tilde{h}(0) = -\tilde{h}(1) = \frac{1}{\sqrt{2}}$ . Haar basis is unique, since it is the only wavelet, which is symmetric and compactly supported. In a level one Haar wavelet decomposition, the level-I low-pass (average) and high-pass (wavelet or detail) coefficients are respectively given by the nearest neighbor averages and differences, with the normalization factor of  $\frac{1}{\sqrt{2}}$ . In the subsequent step, the average coefficients are divided into two parts, containing level-II high-pass and level-II low-pass coefficients. The high-pass coefficients now represent differences of averaged data points corresponding to a window size of two. Wavelets belonging to Daubechies family are designed such that, the wavelet coefficients are independent of polynomial trends in the data. For example, Daubechies-4 wavelet satisfies,  $\int t\psi(t)dt = 0$ , in addition to all other conditions. Because of this the wavelet coefficients here capture fluctuations over and above the linear variations. For Daubechies-4,  $h(0) = -\tilde{h}(3) = \frac{1+\sqrt{3}}{4\sqrt{2}}$ ,  $h(1) = \tilde{h}(2) = \frac{3+\sqrt{3}}{4\sqrt{2}}$ ,  $h(2) = -\tilde{h}(1) = \frac{3-\sqrt{3}}{4\sqrt{2}}$ ,  $h(3) = -\tilde{h}(0) = \frac{1-\sqrt{3}}{4\sqrt{2}}$ . We have used both Haar and Daubechies-4 wavelets for isolating these fluctuations at different scales and study their character. For continuous wavelet transform (CWT), we have utilized Morlet wavelet, whose analyzing function is given by,

$$\psi(t) = \pi^{-1/4} e^{(-i\omega_0 t - t^2/2)}. \quad (2)$$

The corresponding wavelet coefficients are displayed as a function of scale and time in a scalogram.

In DWT, a maximum of  $N$  level decompositions can be carried out, when the data set is of size  $2^N$ . One may choose to have a less number of decompositions than  $N$ . Often one needs to supplement the data with additional points to carry out a  $N$  level decomposition. Both in DWT and CWT, one encounters boundary artifacts, due to circular or other forms of extensions. In our case, for minimizing these boundary artifacts, we have used symmetric extension, while studying the behavior of wavelet coefficients. The variations at different scales are characterized by their respective powers, defined as the squared sum of the wavelet coefficients at that level. Since in wavelet transform power is conserved, the squared sum of all the low pass and high pass coefficients add up to the squared sum of the data points of the time series, called as the total power or energy. We have used normalized power which is the power at a given level divided by the total power. Periodic extension has been used for analyzing the distribution of power at various levels, since this extension conserves power. The power plots depicting high pass power and low pass power clearly reveal the character of the fluctuation and the average behavior.

We start with the National Stock Exchange (NSE) of India Nifty daily closing index values, consisting of 2048 data points, covering the duration from 24<sup>th</sup> December 1997 to 16<sup>th</sup> February 2006. This daily index is shown in Fig. 1. We carry out an eight level decomposition through Haar transform, since the same yields a transparent picture about the nature of the variations. The high pass coefficients are depicted in Fig. 2. Transient and cyclic behavior at different scales are clearly visible. The corresponding low pass coefficients corresponding to 8<sup>th</sup> level are depicted in Fig. 3. As expected, these low pass coefficients capture the average behavior of the time series (see Fig. 1). At finer resolutions corresponding to lower level wavelet coefficients, one can clearly see primarily random nature of the fluctuations.

The non-random variations significantly increase from 6<sup>th</sup> level onwards. Substantial increase in power at 6<sup>th</sup> level is also evident in Fig. 4, which shows the behavior of the normalized power of the high pass coefficients. The normalized power of low pass coefficients shown in Fig. 5 start decreasing from 6<sup>th</sup> level onwards, since the total power is conserved in wavelet transform. It is worth mentioning that the 6<sup>th</sup> level high pass coefficients correspond to the differences of data points, averaged over a temporal window size 32. A few transient phenomena are also revealed by these coefficients. After sufficient averaging, cyclic behavior is seen to emerge. The averaged low pass coefficients reveal a linear trend like the time series in Fig. 1; this can affect the high pass coefficients. In order to remove this and capture the characteristic nature of the variations, we have carried out decomposition through Daubechies-4 wavelets. The structured and cyclic behavior is transparently demonstrated in Fig. 6. This justifies the use of Daubechies-4 wavelets, which removes linear trend from the high-pass coefficients. Plots of both high-pass and low-pass normalized power reveal that at higher

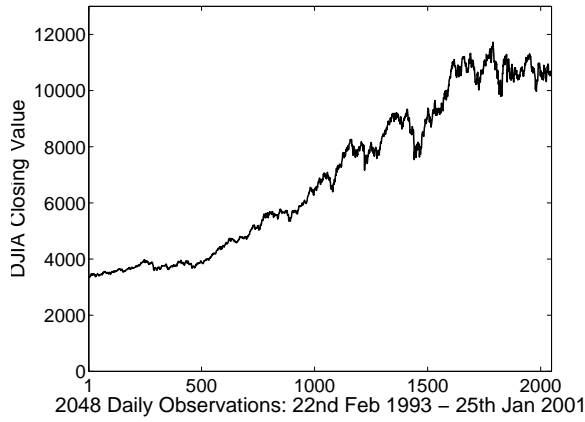


FIG. 9: DJIA closing values having 2048 points covering the daily index lying within 22-Feb-1993 to 25-Jan-2001.

scales fluctuations capture most of the energy; the high-pass power increases, while that of low-pass decreases progressively. CWT through Morlet wavelets also reveal the cyclic behavior at intermediate scales as seen in Fig. 7. The scale values indicate the window size of the Morlet wavelet corresponding to the same number of days. We depict in Fig. 8 sum over the continuous wavelet coefficients over scales as a function of time. An approximate periodic behavior is seen with a period of about 200 trading days. The fact that wavelet coefficients containing both positive and negative values add up to yield a periodic behavior indicates the presence of correlated behavior. As is clear, purely random un-correlated coefficients will not lead to this structure.

We next consider the Dow Jones industrial average (DJIA) closing values, shown in Fig. 9 having 2048 data points for the duration lying within 22<sup>nd</sup> February 1993 to 25<sup>th</sup> January 2001. An eight level decomposition through Haar transform is then carried out to infer about the nature of the variations. The high pass coefficients are depicted in Fig. 10. Transient and cyclic behavior at different scales are clearly visible like the previous case of Nifty data. It is to be noted that the 2<sup>nd</sup> half of the forward wavelet coefficients for each level is having higher amplitudes as compared to the first half of the coefficients. In this respect, variations of wavelet coefficients of Nifty data and DJIA data have different characteristics. The corresponding low pass coefficients are shown in Fig. 11. As is evident, these low pass coefficients show the trend of the time series. The normalized power of the high pass coefficients (Fig. 12) shows a continuous rise with levels having a small decline at level 8. Correspondingly the low pass coefficients show continuous decrease in the power (Fig. 13). In Fig. 14 we show the Db4 wavelet coefficients for levels 1 to 8 for the purpose of comparison with the corresponding Nifty index behavior.

We have studied the behavior of DJIA under CWT. The corresponding scalogram is shown in Fig. 15. Akin to the Nifty case one sees cyclic behavior in the scale

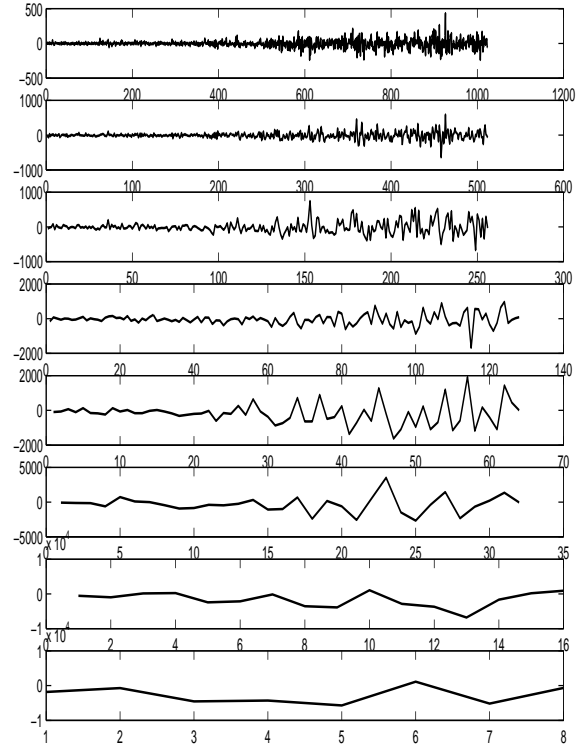


FIG. 10: Haar wavelet coefficients for levels 1 to 8 for Dow Jones data.

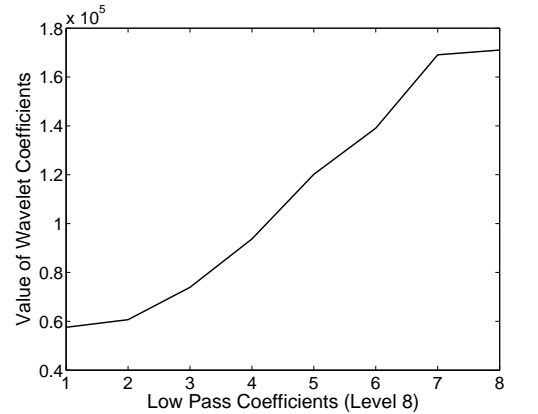


FIG. 11: Haar wavelet low pass coefficients for levels 1 to 8 for Dow Jones data. A linear trend is seen.

range 100 to 200. The sum of the wavelet coefficients at all scales plotted as a function of time (Fig. 16) reveal a periodic behavior of little less than 200 trading days. In this context both the financial time series show similar behavior. However the DJIA time series is showing a tendency of bursty behavior which is absent in Nifty case.

Considering the cyclic behavior of variations at intermediate scales, it is interesting to see how well these wavelet coefficients can be analyzed through the techniques of Genetic Programming in which the model equations are built in the reconstructed phase space. This modeling can reveal characteristic behavior of fluctua-

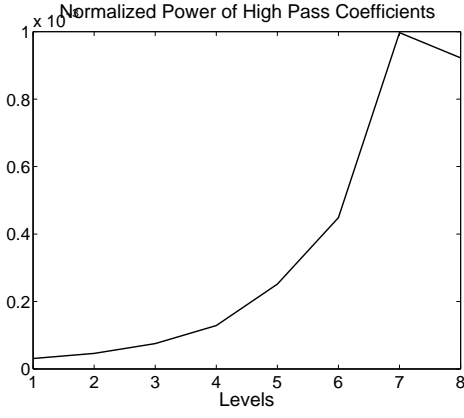


FIG. 12: Normalized power of Haar wavelet high pass coefficients for levels 1 to 8 for Dow Jones data. Significant increase in power is seen around 6<sup>th</sup> level.

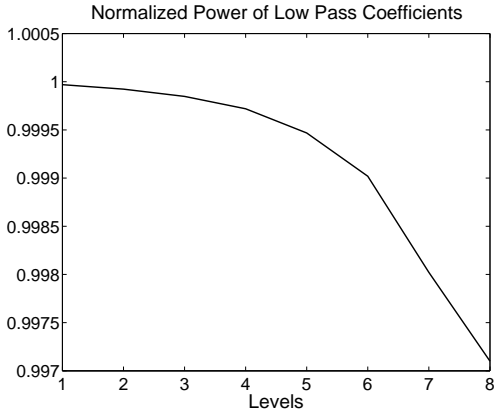


FIG. 13: Normalized power of Haar wavelet low pass coefficients for levels 1 to 8 for Dow Jones data. Complimenting the high-pass behavior, the low-pass power decreases rapidly from 6<sup>th</sup> level onwards.

tions at different scales.

### III. MODELING CYCLIC WAVELET COEFFICIENTS THROUGH GENETIC PROGRAMMING

In Genetic Programming one assumes the map equation relating time lagged variables with the entity  $X_{t+1}$  to be of the form [15, 25],

$$X_{t+1} = f(X_t, X_{t-\tau}, X_{t-2\tau}, \dots, X_{t-(d-1)\tau}) \quad (3)$$

Here  $f$  represents a function involving time series values  $X_t$  in the immediate past and arithmetic operators ( $+$ ,  $-$ ,  $\times$  and  $\div$ ). The numbers appearing in function  $f$  are bounded between the range  $[-N, N]$ , where  $N$  is an integer number, we have chosen  $N$  to be 10. The numbers within the above range are generated with the precision of 1 digit after decimal point. In the above equation,  $d$  represents the number of previous time series values that may appear in the function and  $\tau$  represents a time delay.

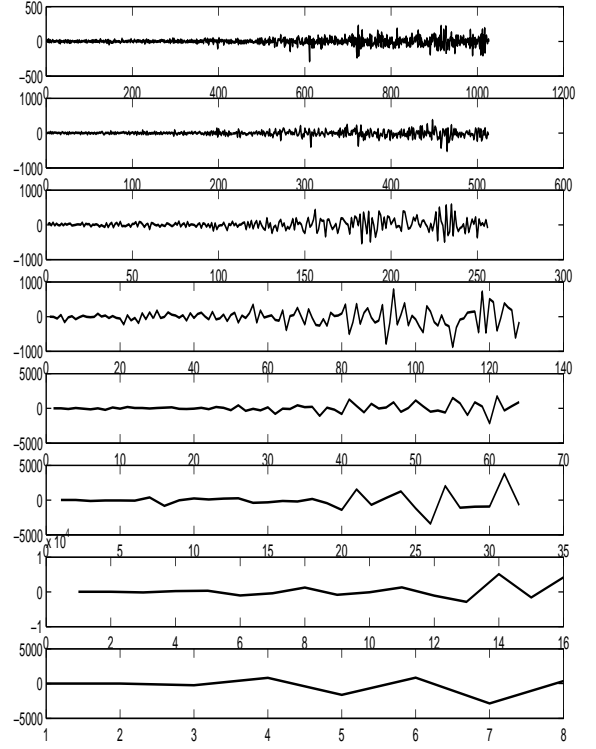


FIG. 14: Db4 wavelet coefficients for levels 1 to 8 for Dow Jones data. Significant activity is seen in the second half of the wavelet coefficients.

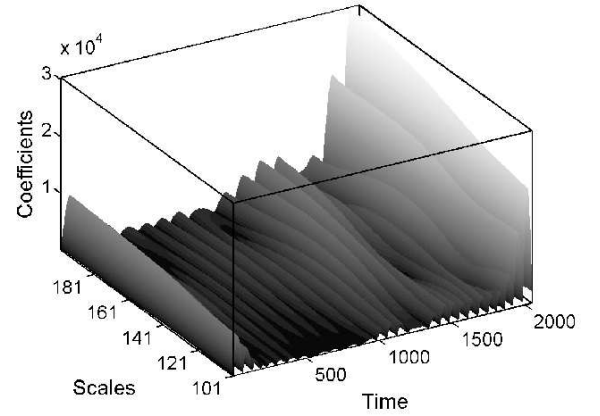


FIG. 15: Scalogram of Morlet Wavelet coefficients for scales 101-200 of DJIA closing values indicating a cyclic behavior.

During the GP optimization, one considers a pool of chromosomes. A chromosome represents a potential solution. Evolution to successive generations is then carried out stochastically by applying genetic operators, namely copy, crossover and mutation.

The sum of squared errors,

$$\Delta^2 = \sum_{i=1}^{i=N} (X_i^{calc} - X_i^{given})^2, \quad (4)$$

is minimized, where  $N$  represents number of  $X_t$  values (Eq. 3) that are fitted during the GP optimization.

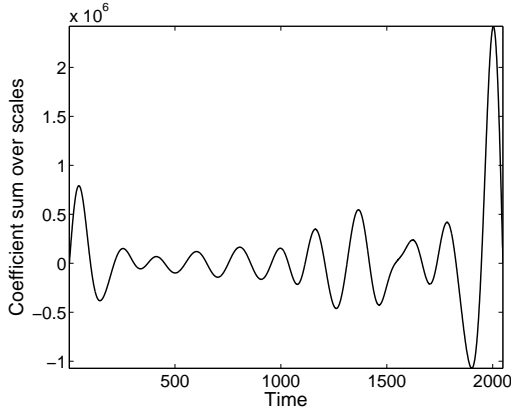


FIG. 16: Sum of wavelet coefficients for DJIA over all scales as a function of time. An approximate cyclic behavior with periodicity of a duration of little less than 200 trading days is evident.

For a given chromosome, the lower the above sum of squared errors, the better is the fit generated and therefore the corresponding chromosome fairs better chance of participating in further evolutionary process through its fitness measure. The fitness measure is derived from  $\Delta^2$  and is defined as in Eq. 5:

$$R^2 = 1 - \frac{\Delta^2}{\sum_{i=1}^N (X_i^{given} - \overline{X_i^{given}})^2}, \quad (5)$$

where  $\overline{X_i^{given}}$  is the average of all  $X_i$  (Eq. 3) to be fitted.

It is observed that during the optimization process, in order to get higher and higher fitness measures, GP may lead to quite involved chromosome strings. In order to discourage GP to over fit by generating longer strings of chromosomes, the fitness measure is modified [15] as follows,

$$r = 1 - (1 - R^2) \frac{N - 1}{N - k}, \quad (6)$$

where  $N$  is the number of equations to be fitted in the training set and  $k$  is the total number of time lagged variables of the form  $X_t, X_{t-\tau}, X_{t-2\tau}, \dots$  etc (including repetitions) occurring in the given chromosome. This modified fitness measure prefers a parsimonious model by generating crisp map equations for chromosomes. For  $R^2$  close to 0, the modified fitness measure  $r$  can be negative.

The map equations generated by above GP prescription is then used to make out-of-sample predictions outside the fitted set of data and the measure of goodness of predictions is ascertained by normalized mean square error (NMSE) as given by Eq. 7,

$$NMSE = \frac{1}{N} \frac{\sum_{i=1}^{i=N} (X_i^{calc} - X_i^{given})^2}{\text{variance of } N \text{ data points}} \quad (7)$$

On trying to model these wavelet coefficients, it is found that due to sharp variations, the GP optimization does not lead to convergence having good fitness

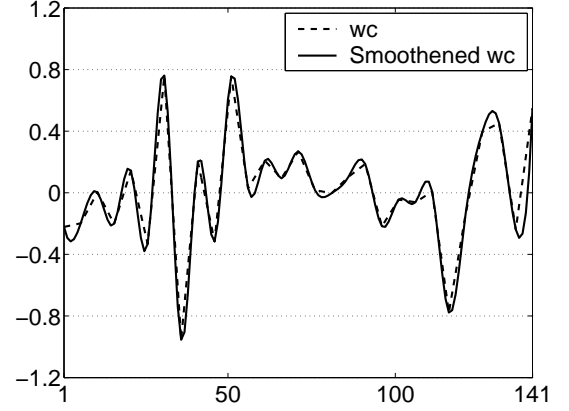


FIG. 17: Db4 wavelet coefficients (wc) and Spline interpolated wc for 6<sup>th</sup> level for Nifty data.

values. We have therefore found it necessary to smoothen these wavelet coefficients using an appropriate method. For all the wavelet coefficients of different levels considered, we smoothen them using a cubic Spline interpolation method. We generate smoothened coefficients by incorporating 4 additional points which are sampled by cubic Spline method for each consecutive pair of points. The piecewise polynomial form of the smoothened data is well suited with a similar structure used for the map equation (Eq. 3) searched by Genetic Programming. It is worth emphasizing that this procedure is appropriate since we are modeling cyclic behavior which are generally smooth in nature as compared to sharp variations of transients.

We now proceed with modeling of smoothened Db4 forward wavelet coefficients using GP at level=6, 7 and 8.

#### A. Modeling variations in S&P CNX Nifty closing index

As seen earlier cyclic and structured variations emerge at relatively higher scales. For modeling purpose, we consider the 6, 7 and 8<sup>th</sup> level coefficients generated using Db4 forward wavelet transform. These coefficients show considerable cyclic fluctuations both at local and global scales. At 6<sup>th</sup> level, bursty behavior is also seen.

We have divided the values of these wavelet fluctuations by 1000 for the sake of computational convenience. The smoothened wavelet coefficients for level=6, 7 and 8 are shown in Figs. 17, 18 and 19 along with original wavelet coefficients.

The smoothened wavelet coefficients are then modelled using GP. We have used  $d=5$  and  $\tau=1$  for these fits and the resulting fits are very good having fitness values 0.99499 (level=6), 0.99498 (level=7) and 0.997038 (level=8).

The map equations are shown in Eq. 8, 9 and 10.

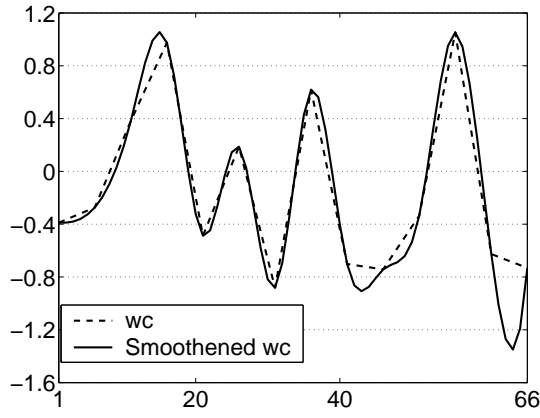


FIG. 18: Db4 wavelet coefficients (wc) and Spline interpolated wc for 7<sup>th</sup> level for Nifty data.

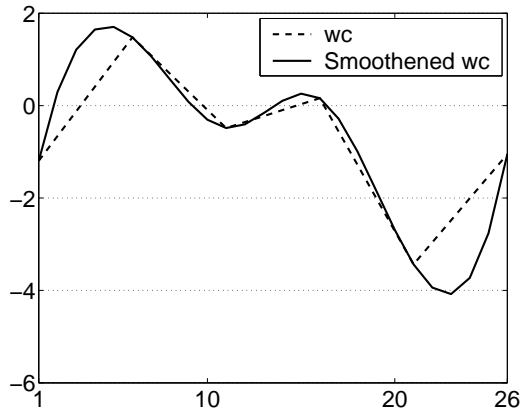


FIG. 19: Db4 wavelet coefficients (wc) and Spline interpolated wc for 8<sup>th</sup> level for Nifty data.

$$\begin{aligned}
 X_{t+1}^{(Level=6)} &= 1.9762X_t + \frac{2.5298X_t}{X_{t-2\tau} + 10.0} - 1.5627X_{t-\tau} + 0.3008X_{t-3\tau} \\
 &+ \frac{0.0006023X_{t-2\tau}}{X_{t-4\tau} - 0.0339} \quad (8)
 \end{aligned}$$

$$X_{t+1}^{(Level=7)} = 2.814X_t - 2.9401X_{t-\tau} + 1.1239X_{t-2\tau} - 0.01761X_{t-3\tau} \quad (9)$$

$$X_{t+1}^{(Level=8)} = 1.5X_t - 0.6522X_{t-2\tau} - \frac{0.368(X_{t-\tau} - 2.9X_{t-4\tau} + 1.3103)}{2.4X_t + 3.18} \quad (10)$$

The GP fit obtained by these equations are quite good and these are shown for level=6, 7 and 8 in Figs. 20, 21 and 22 respectively.

The goodness of the fits is indicated by the small values of the differences between given and calculated values shown by the line close to 0.0.

It is worth pointing out that the GP map equations representing cyclic variations are primarily found to be linear. The nonlinearity if any, arising from the Padé

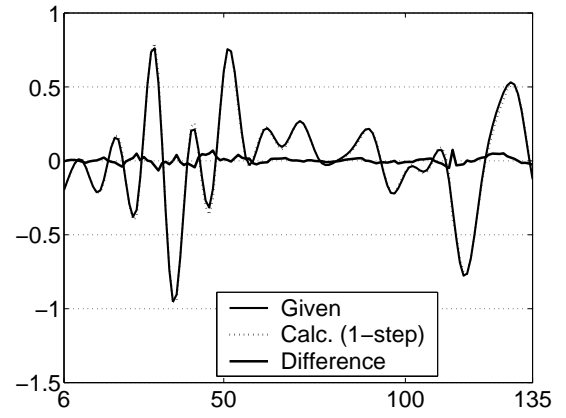


FIG. 20: Fit for 130 data points using GP solution for Db4 level-6 wavelet coefficients for Nifty data.

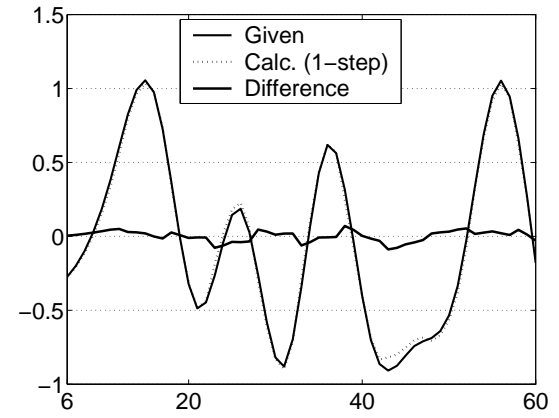


FIG. 21: Fit for 55 data points using GP solution for Db4 level-7 wavelet coefficients for Nifty data.

type rational terms, has rather small coefficients as compared to those for the linear terms. It is also noted that the significant departure of the obtained solutions from a persistent solution ( $X_{t+1}=X_t$ ) shows the efficacy of the GP optimization approach. In the context of specific lev-

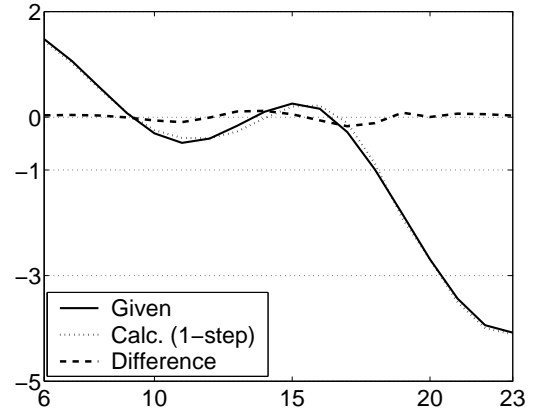


FIG. 22: Fit for 18 data points using GP solution for Db4 level-8 wavelet coefficients for Nifty data.



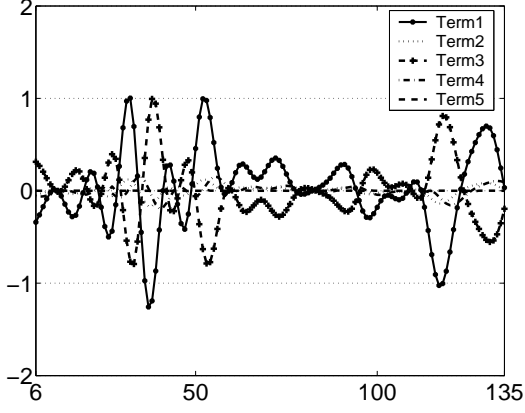


FIG. 23: Contributions of individual terms in the right hand side of Eq. 8 for Db4 level-6 wavelet coefficients for Nifty data. It is observed that the first and third terms are the dominant ones which give rise to the bursty behavior (Fig. 20) due to their slight out of phase dynamics.

els, we observe that the 6<sup>th</sup> level variations show cyclic as well as bursty behavior. Interestingly, the 7<sup>th</sup> level coefficients show smooth variations; the corresponding GP equation (Eq. 9) is completely linear. On the contrary the 8<sup>th</sup> level variations show non-smooth variations which are not bursty like the 6<sup>th</sup> level coefficients.

In order to understand the interplay of different terms giving rise to the bursty behavior, we have computed the contributions arising from each term of Eq. 8 individually. The same is shown in Fig. 23. It is clearly seen that the first and the third term are the dominant ones, which are slightly out of phase from each other. The corresponding cancellation is responsible for the bursty behavior. The dynamical origin of these terms and their modeling is rather non-trivial, which needs significant investigations.

The map equations will now be used to carry out 1-step out-of-sample predictions beyond the fitted points. The predictions for level=6, 7 and 8 are shown in Figs. 24, 25 and 26 respectively with corresponding NMSE values as 0.04923, 0.03907 and 0.03946 respectively. It can be seen that the 1-step predictions are very good.

### B. Modeling variations in Dow Jones Industrial Average Closing values

We next consider modeling of Db4 wavelet coefficients for Dow Jones Industrial Average (DJIA) closing values. Akin to the GP analysis for Nifty wavelet coefficients, we have found it useful to smoothen the wavelet coefficients using Cubic Spline for the purpose of GP modeling. This also makes it easier to compare the cyclic variations in the two time series considered

The comparison of Db4 forward wavelet coefficients for level=6, 7 and 8 with the Cubic Spline smoothened coefficients are shown in Figs. 27, 28 and 29.

The map equations generated by GP for  $d=5$  and  $\tau=1$

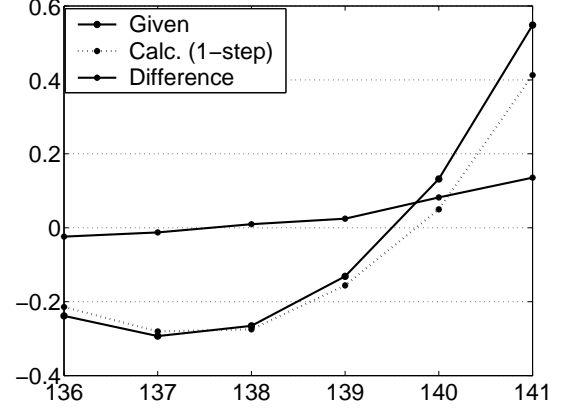


FIG. 24: Out-of-sample 1-step predictions using GP solution for Db4 level-6 wavelet coefficients for Nifty data.

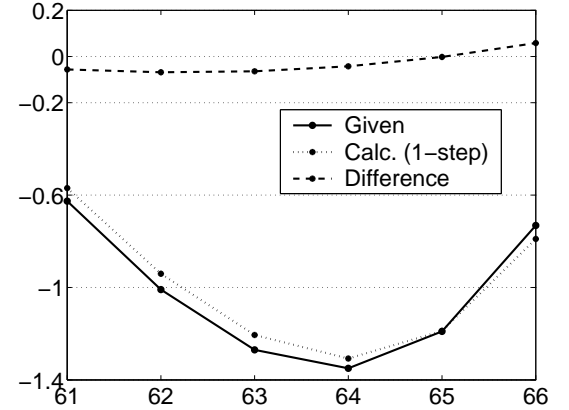


FIG. 25: Out-of-sample 1-step predictions using GP solution for Db4 level-7 wavelet coefficients for Nifty data.

are having fitness values 0.998013, 0.99721, and 0.99929 and are shown in Eq. 11, 12 and 13.

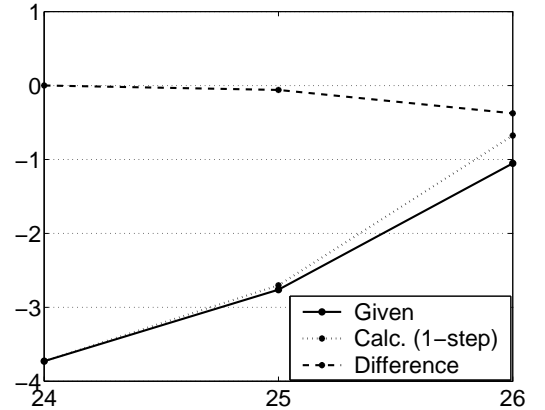


FIG. 26: Out-of-sample 1-step predictions using GP solution for Db4 level-8 wavelet coefficients for Nifty data.

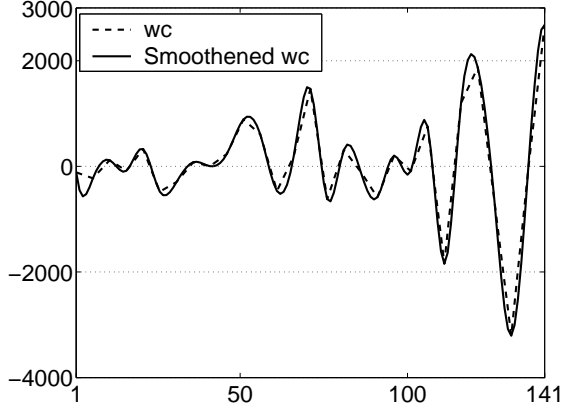


FIG. 27: Db4 wavelet coefficients (wc) and Spline interpolated wc for 6<sup>th</sup> level Dow Jones data.

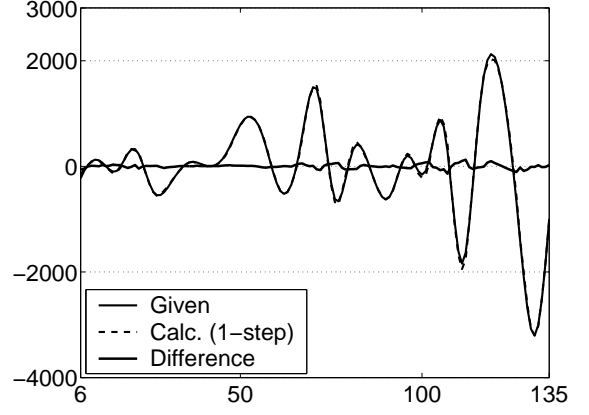


FIG. 30: Fit of the GP solution for Db4 level-6 Dow Jones wavelet coefficients. The variations have a bursty character.

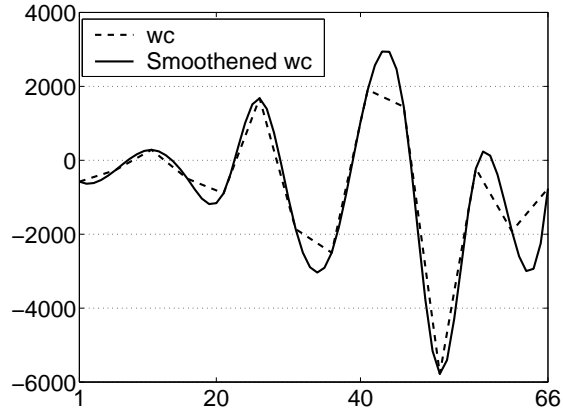


FIG. 28: Db4 wavelet coefficients (wc) and Spline interpolated wc for 7<sup>th</sup> level Dow Jones data.

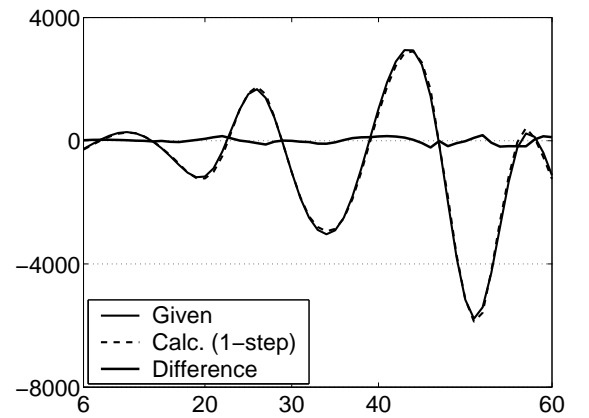


FIG. 31: Fit of the GP solution for Db4 level-7 Dow Jones wavelet coefficients. The amplitude of the cyclic variations is seen to increase with time.

$$\begin{aligned}
 X_{t+1}^{(Level=6)} = & 2.4375X_t - 1.8398X_{t-\tau} + 0.12669X_{t-2\tau} + 0.2587X_{t-3\tau} \\
 & + 0.7002 + \frac{0.0186(X_{t-4\tau} + 248.5)}{X_{t-\tau}} \\
 & + \frac{0.6841(1.5X_t + 125.85)}{X_{t-4\tau} + 76.3}
 \end{aligned} \quad (11)$$

$$\begin{aligned}
 X_{t+1}^{(Level=7)} = & 2.2386X_t - 1.5X_{t-\tau} + 0.0947X_{t-2\tau} + 0.1481X_{t-4\tau} \\
 & - 16.993 - \frac{0.71023(X_{t-\tau} + 540.519)}{X_{t-2\tau} - X_{t-3\tau}}
 \end{aligned} \quad (12)$$

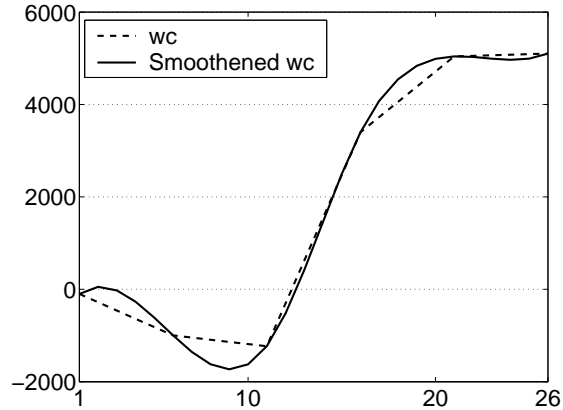


FIG. 29: Db4 wavelet coefficients (wc) and Spline interpolated wc for 8<sup>th</sup> level Dow Jones data.

$$\begin{aligned}
 X_{t+1}^{(Level=8)} = & 2.20989X_t - 1.3999X_{t-\tau} + 0.16484X_{t-3\tau} + 62.9235 \\
 & - \frac{0.10989X_{t-\tau}}{X_{t-3\tau}}
 \end{aligned} \quad (13)$$

As seen in Figs. 30, 31 and 32 for level=6, 7 and 8 respectively, the GP fits are quite good.

Similar to the Nifty analysis, the GP equations are primarily of linear type having non-linear terms of Padé type. Eq. 11 is primarily linear. The effect of nonlinearity as seen from the Padé terms is different from the Nifty behavior. Eq. 12 shows a very interesting behavior. If difference between two consecutive data points are small, then the Padé term gives a strong contribution, which decreases as the differences increase. Eq. 13 representing level 8 coefficients is again mostly linear.

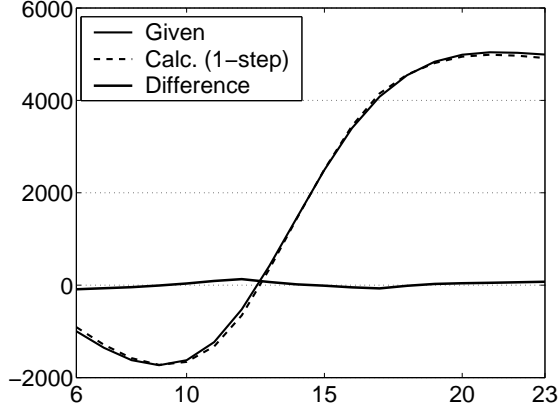


FIG. 32: Fit of the GP solution for Db4 level-8 Dow Jones wavelet coefficients. The variations show a step like behavior.

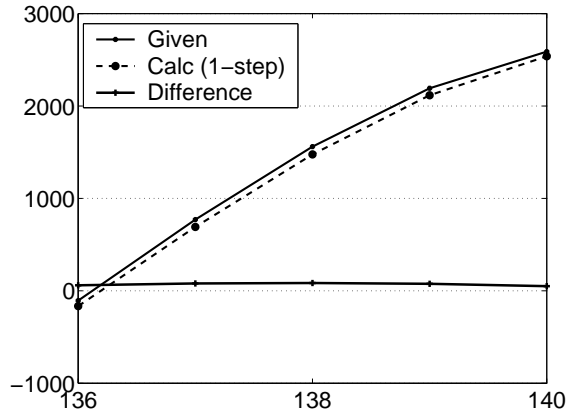


FIG. 33: Out-of-sample 1-step predictions using GP solution for Db4 level-6 Dow Jones wavelet coefficients.

We then use these map equations and carry out 1-step out-of-sample predictions beyond the fitted points. These predictions are found to be very good as is reflected from their small NMSE values, 0.001787 (level=6), 0.002379 (level=7) and 0.0004981 (level=8). The predictions are shown for level=6, 7 and 8 in Figs. 33, 34 and 35 respectively and are found to be excellent.

#### IV. CONCLUSION

In conclusion, we have illustrated a wavelet based approach to separate stochastic and structured variations in non-stationary time series. Modeling different aspects e.g., fluctuations and trend of these time series is a challenging task. It becomes particularly difficult when the fluctuations comprise of random, cyclic and transient variations at multiple scales. The fact that wavelet transform possesses multi-resolution analysis capability, has opened the way to isolate variations at different scales.

We have taken advantage of this ability of wavelets to study and model cyclic variations of the financial time series, which are known to be non-stationary. Genetic

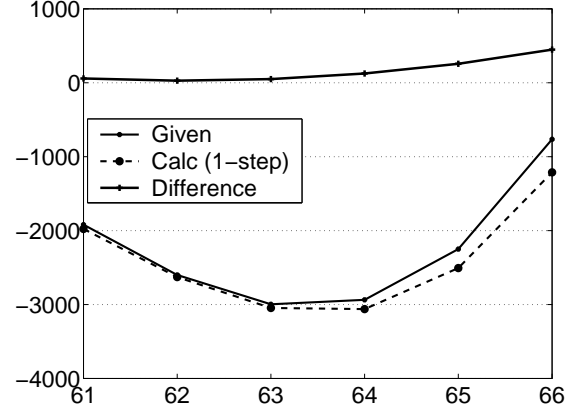


FIG. 34: Out-of-sample 1-step predictions using GP solution for Db4 level-7 Dow Jones wavelet coefficients.

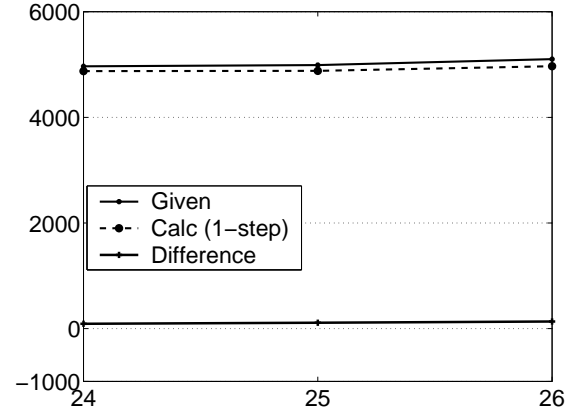


FIG. 35: Out-of-sample 1-step predictions using GP solution for Db4 level-8 Dow Jones wavelet coefficients.

programming models the cyclic behavior well through crisp dynamical equations. One step predictions have been carried through and these are found to be quite accurate.

Apart from studying other physical time series, it will be nice to combine the present approach with random matrix based ones for the purpose of pinpointing emergence of cyclic behavior. As has been mentioned earlier, random matrix approach has indicated correlation between group of companies in financial time series, which can lead to cyclic or structured variations apparent in the present analysis. Hence, it will be of deep interest to see if these two can be interrelated.

Amit Verma is thankful to Physical Research Laboratory for providing him a project traineeship during which part of this work was done.

- Econophysics: Correlations and Complexity in Finance* (Cambridge University Press, 2000).
- [3] M. G. Mankiw, D. Romer and M. D. Shapiro, *Stock Market forecastability and volatility: a statistical appraisal* Review of Economic Studies, **58**, 455 (1997).
  - [4] J. B. Ramsey, D. Usikov and G. Zaslavsky, *Fractals* **3**, 377 (1995).
  - [5] P. C. Biswal, B. Kamaiah and P. K. Panigrahi, *Jou. of Quant. Econ.* **2**, 133 (2004).
  - [6] M. Schulz, S. Trimper and B. Schulz, *Phys. Rev. E* **64**, 026104-1 (2001).
  - [7] V. Plerou, P. Gopikrishnan, B. Rosenow, L. A. N. Amaral and H. E. Stanley, *Phys. Rev. Lett.* **83** 1471 (1999); L. Laloux *et al.*, *Phys. Rev. Lett.*, **83**, 1467 (1999).
  - [8] K. B. K. Mayya, R. E. Amritkar, and M. S. Santhanam, *Delay Correlation and Random Matrices*, submitted for publication.
  - [9] I. Daubechies *Ten Lectures on Wavelets*, Vol. 64 of CBMS-NSF Regional Conference Series in Applied Mathematics, Society of Industrial and Applied Mathematics, Philadelphia (1992).
  - [10] R. Gencay, F. Selcuk and Whitcher *An Introduction to Wavelets and Other Filtering Methods in Finance and Economics* (Academic Press, 2001).
  - [11] J. H. Holland, *Adaptation in Natural and Artificial Systems* (University of Michigan Press, Ann Arbor 2<sup>nd</sup> ed, 1975).
  - [12] D. E. Goldberg, *Genetic Algorithms in Search, Optimization, and Machine Learning* (Addison Wesley publication, 1989).
  - [13] D. B. Fogel, *Evolutionary Computation, The Fossil Record*, (IEEE Press, 1998).
  - [14] M. Mitchell, *An Introduction to Genetic Algorithms* (MIT Press, 1996).
  - [15] G. G. Szpiro, *Phys. Rev. E* **55**, 2557 (1997).
  - [16] P. M. Manimaran, P. K. Panigrahi, and J. C. Parikh, *Phys. Rev. E* **72**, 046120 (2005); P. M. Manimaran, P. K. Panigrahi, and J. C. Parikh, *Multiresolution Analysis of Stock Market Price Fluctuations*, e-print: nlin.CD/0601074 and references therein; P. M. Manimaran, J. C. Parikh, P. K. Panigrahi, S. Basu, C.M. Kishtewal and M.B. Porecha, *Econophysics of Stock and Other Markets*, edited by A.Chatterjee and B.K.Chakrabarti, Springer-Verlag, Italy, 183 (2006).
  - [17] D. Percival and A. Walden, *Wavelet Analysis for Time Series Analysis*, (Cambridge University Press, 2000).
  - [18] P. K. Clark, *Econometrica*, **41**, 135 (1973).
  - [19] S.-H Poon and C. W. J. Granger, *Jou. of Economics Literature*, **41**, 478 (2003).
  - [20] J. Connor and R. Rossiter, *Studies in Nonlinear Dynamics and Econometrics* **9**, 1 (2005).
  - [21] I. Simonsen, *Physica A* **322**, 597 (2003).
  - [22] J. Karuppiah and C. A. Los, *International Review of Financial Analysis* **14(2)**, 211 (2005).
  - [23] J. B. Ramsey and Z. Zhang, *The Applicability of Waveform Dictionaries to Stock Market data, in Predictability of Dynamic Systems*, edited by Y. Krastov and J. Kadtke, Springer-Verlag, New York, 189 (1996).
  - [24] S. Hayward, *Econophysics of Stock and Other Markets*, edited by A. Chatterjee and B. K. Chakrabarti, Springer-Verlag, Italy, 163 (2006).
  - [25] P. Grassberger and I. Procaccia, *Phys. Rev. Lett.* **50**, 346 (1983).